CellPress
PARTNER JOURNAL

Molecular Plant
Research Article

Two RING-Finger Ubiquitin E3 Ligases Regulate the Degradation of SPX4, An Internal Phosphate Sensor, for Phosphate Homeostasis and Signaling in Rice

Wenyuan Ruan[1], Meina Guo[1], Xueqing Wang[1], Zhenhui Guo[1], Zhuang Xu[1], Lei Xu[1], Hongyu Zhao[1], Haiji Sun[2], Chengqi Yan[3] and Keke Yi[1,*]

[1]Key Laboratory of Plant Nutrition and Fertilizer, Ministry of Agriculture, Institute of Agricultural Resources and Regional Planning, Chinese Academy of Agricultural Sciences, Beijing 100081, China

[2]College of Life Science, Shandong Normal University, Jinan 250014, China

[3]Ningbo Academy of Agriculture Sciences, 19 Dehou Street, Ningbo City 315000, China

***Correspondence: Keke Yi (yikeke@gmail.com)**

https://doi.org/10.1016/j.molp.2019.04.003

ABSTRACT

SPX-domain-containing proteins (SPXs) play an important role in inorganic phosphate (Pi) sensing, signaling, and transport in eukaryotes. In plants, SPXs are known to integrate cellular Pi status and negatively regulate the activity of Pi central regulators, the PHOSPATE STARVATION RESPONSE proteins (PHRs). The stability of SPXs, such as SPX4, is reduced under Pi-deficient conditions. However, the mechanisms by which SPXs are degraded remain unclear. In this study, using a yeast-two-hybrid screen we identified two RING-finger ubiquitin E3 ligases regulating SPX4 degradation, designated SDEL1 and SDEL2, which were post-transcriptionally induced by Pi starvation. We found that both SDELs were located in the nucleus and cytoplasm, had ubiquitin E3 ligase activity, and directly ubiquitinated the K^{213} and K^{299} lysine residues in SPX4 to regulate its stability. Furthermore, we found that PHR2, a Pi central regulator in rice, could compete with SDELs by interacting with SPX4 under Pi-sufficient conditions, which protected SPX4 from ubiquitination and degradation. Consistent with the biochemical function of SDEL1 and SDEL2, overexpression of *SDEL1* or *SDEL2* resulted in Pi overaccumulation and induced Pi-starvation signaling even under Pi-sufficient conditions. Conversely, their loss-of-function mutants displayed decreased Pi accumulation and reduced Pi-starvation signaling. Collectively, our study revealed that SDEL1 and SDEL2 facilitate the degradation of SPX4 to modulate PHR2 activity and regulate Pi homeostasis and Pi signaling in response to external Pi availability in rice.

Key words: rice, SPX4, PHR2, ubiquitination, Pi signaling, Pi homeostasis, phosphate regulation network

Ruan W., Guo M., Wang X., Guo Z., Xu Z., Xu L., Zhao H., Sun H., Yan C., and Yi K. (2019). Two RING-Finger Ubiquitin E3 Ligases Regulate the Degradation of SPX4, An Internal Phosphate Sensor, for Phosphate Homeostasis and Signaling in Rice. Mol. Plant. **12**, 1060–1074.

INTRODUCTION

Plant growth and development are strongly influenced by the availability of phosphorus (P) in natural and agricultural ecosystems. Inorganic phosphate (Pi), the plant-accessible form of P, easily forms insoluble complexes or precipitates with organic matter or mineral cations, which makes it inaccessible to the plant (Kirkby, 2012; Neumann and Römheld, 2012). To optimize crop yield, large quantities of Pi fertilizers, produced from non-renewable phosphate rock, are applied in modern agriculture, resulting in the depletion of global P reserves and the risk of eutrophication (Manning, 2008; Gilbert, 2009). Therefore, developing crop varieties with higher Pi uptake and utilization efficiency is a big challenge for breeders to meet, and requires a deeper understanding of the regulatory mechanisms underlying Pi sensing and signaling in plants.

Published by the Molecular Plant Shanghai Editorial Office in association with Cell Press, an imprint of Elsevier Inc., on behalf of CSPB and IPPE, SIBS, CAS.

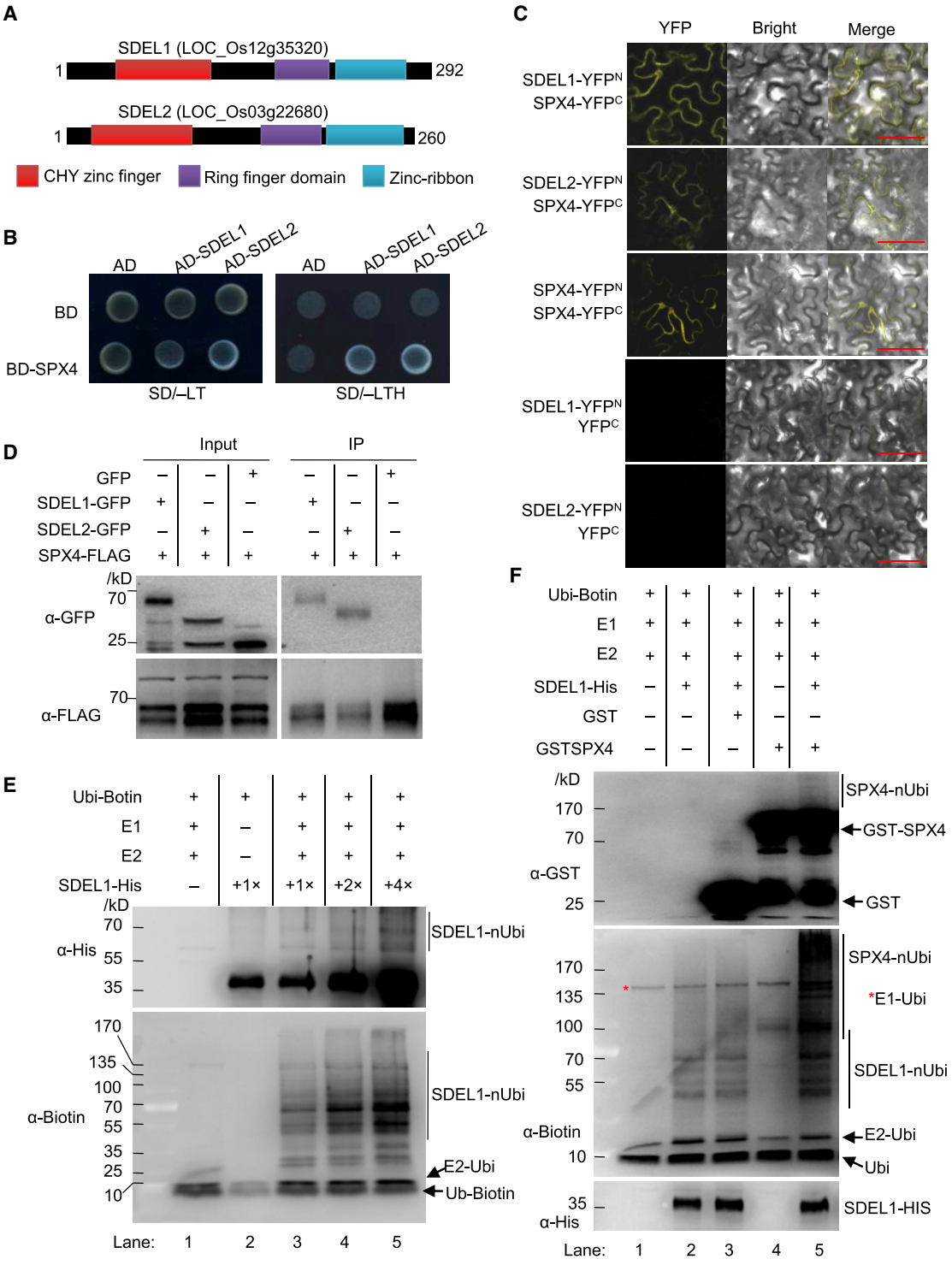

Figure 1. SDEL1 Exhibits E3 Ubiquitin Ligase Activity and Ubiquitinates SPX4.

(A) Schematic of the predicted protein domains of SDEL1 and SDEL2. Red box indicates CHY zinc-finger domain; purple box indicates ring-finger domain; blue box indicates zinc ribbon.

(B) Y2H assay of the interaction of SDEL1/2 and SPX4. SDEL1 and SDEL2 were fused to the GAL4 activation domain to generate AD-SDEL1 and AD-SDEL2. SPX4 was fused to the GAL4 binding domain to generate BD-SPX4. Yeast cells co-transformed with AD-SDEL1/BD-SPX4 or AD-SDEL2/BD-SPX4 were grown on selective media (SD/-LT and SD/-LTH with 10 μM MG132). AD/BD, AD/BD-SPX4, AD-SDEL1/BD, and AD-SDEL2/BD were co-expressed as negative controls.

(C) BiFC analysis of the interaction between SDEL1/2 and SPX4. N-terminal fragment of YFP (YFP^N) was fused to the C terminus of SDEL1, SDEL2, and PHR2. C-terminal fragment of YFP (YFP^C) was fused to SPX4. The combination SPX4-YFP^N/SPX4-YFP^C was used as a positive control. Scale bars, 20 μm.

(legend continued on next page)

PHOSPHATE STARVATION RESPONSE proteins (PHRs) are the central regulators of Pi signaling in plants. They play a pivotal role in regulating Pi-starvation responses by binding to the *cis* element P1BS (PHR1 binding site, GNATATNC) in the promoters of Pi-starvation induced (PSI) genes in plants (Rubio et al., 2001; Valdés-López et al., 2008; Zhou et al., 2008; Bustos et al., 2010; Ren et al., 2012; Wang et al., 2013; Guo et al., 2015; Ruan et al., 2017). For example, PHRs can directly bind to the promoters of PHOSPHATE TRANSPORTERs (PHTs) to regulate the uptake of Pi from Pi translocation or Pi derived from external sources in different tissues (Bustos et al., 2010; Liu et al., 2010). In addition, PHRs also directly regulate the expression of *miRNA399* and *miRNA827*, and thus indirectly modulate the expression of the targets of these microRNAs (miRNA), *PHO2* and *NLA* (ubiquitin system components), respectively, to regulate Pi homeostasis and Pi signaling (Zhou et al., 2008; Bustos et al., 2010; Kant et al., 2011; Liu et al., 2012; Lin et al., 2018).

The transcriptional activities of PHRs are negatively regulated solely by SPX (named after SYG1 [suppressor of yeast gpa1], Pho81 [CDK inhibitor in yeast PHO pathway], and XPR1 [xenotropic and polytropic retrovirus receptor])-domain-containing proteins (SPXs) (Duan et al., 2008; Liu et al., 2010; Lv et al., 2014; Puga et al., 2014; Shi et al., 2014; Wang et al., 2014; Zhong et al., 2018). SPXs are found throughout the eukaryotic tree of life, including in fungi, plants, and metazoans (Secco et al., 2012a, 2012b; Wild et al., 2016). A recent study has confirmed that SPXs can sense Pi status, as the basic surface on the SPX domain can bind to Pi at low affinity and to inositol pyrophosphates (IPs) at high affinity (Wild et al., 2016). The presence of high concentrations of Pi or low concentrations of IPs can stabilize the interaction of SPXs with a multitude of proteins to regulate Pi transport and signaling (Lv et al., 2014; Wild et al., 2016).

In plants there are four subfamilies of SPXs, namely SPX-EXS (named after the *Saccharomyces cerevisiae* Erd1, mammalian Xpr1, and *S. cerevisiae* Syg1), SPX-MFS (Major Facilitator Superfamily), SPX-RING (Really Interesting New Gene), and SPXs (small proteins with only the SPX domain) (Secco et al., 2012b; Jung et al., 2018). In *Arabidopsis*, SPX-EXS proteins such as AtPHO1 are involved in Pi-signal transduction and transfer Pi from the root to the shoot by exporting Pi out of the stele cells and into the xylem vessel apoplast (Poirier et al., 1991; Hamburger et al., 2002). AtPHO1 is degraded by PHO2 under Pi-sufficient conditions (Liu et al., 2012). The tonoplast-located SPX-MFSs (AtVPT1 in *Arabidopsis* and OsSPX-MFS1 in rice) play a role in exporting Pi from the cytoplasm to the vacuole when Pi is sufficient (Wang et al., 2012; Liu et al., 2015, 2016). Unlike other SPX-containing proteins, SPX-RING proteins encode ubiquitin E3 ligases, such as AtNLAs (NITROGEN LIMITATION ADAPTATION) and OsNLAs. Both *Arabidopsis* and rice *NLA* loss-of-function mutants exhibit Pi overaccumulation phenotypes (Kant et al., 2011; Yang et al., 2017; Yue et al., 2017). Of the proteins that only possess an SPX domain (four members in *Arabidopsis*, AtSPX1–AtSPX4; six in rice, OsSPX1–OsSPX6), physical interaction with PHRs under Pi-sufficient conditions prevents the binding of PHRs to the promoters of PSI genes, thus inhibiting the transcription activity of PHRs (Lv et al., 2014; Puga et al., 2014; Wang et al., 2014; Zhong et al., 2018). In rice, the interaction of OsSPX4 (hereafter SPX4) with OsPHR2 (hereafter PHR2) can be stabilized in the presence of 15 mM Pi or 20 μM IP7 (Lv et al., 2014; Wild et al., 2016). SPX4 inhibits the binding of PHR2 to its *cis* element and reduces the targeting of PHR2 to the nucleus. SPX4 is a fast-turnover protein and its degradation is accelerated under Pi deficiency (Lv et al., 2014). Therefore, the stability of SPX4 is important for Pi signaling. However, the mechanism of degradation of the negative regulator SPX4 is still unknown.

To acquire deeper insight into the degradation mechanism of SPXs in rice, we identified two SPX4 degradation E3 ligases (SDEL1 and SDEL2), which are RING-finger domain- containing E3 ligases. SDEL1 and SDEL2 directly interact with and ubiquitinate SPX4. PHR2 competes with SDEL1 to interact with SPX4 and blocks the binding domain recognized by SDEL1 under Pi-sufficient conditions, thus protecting SPX4 from degradation. Therefore, SDEL1 and SDEL2 and PHR2 co-regulate the stability of SPX4 to adapt to Pi availability in the environment.

RESULTS

SDEL1 and SDEL2 Exhibit E3 Ubiquitin Ligase Activity and Ubiquitinate SPX4

As SPXs are conserved throughout the plant kingdom (Secco et al., 2012a, 2012b) and their stabilities are regulated by external Pi availability (Liu et al., 2012; Lv et al., 2014; Zhong et al., 2018), we hypothesized that ubiquitin E3 ligases could specifically recognize SPXs and regulate their degradation in plants. To screen for candidate E3 ligases that target SPX4, we employed the yeast-two-hybrid (Y2H) system. A chimeric bait vector, SPX4-BD, was used to screen a cDNA library derived from rice roots. Multiple independent cDNAs encoding a putative E3 ligase (Os12g35320; designated SDEL1) were identified from the screen. Bioinformatics analysis showed that SDEL1 is a putative CHY zinc-finger and RING-finger domain-containing E3 ligase and has five homologous proteins encoded in the rice genome (Figure 1A and Supplemental Figure 1). SDEL1 and its homologous protein SDEL2 are expressed in the leaf, root, shoot, anther, and panicle, similar to the expression pattern of

(D) Co-IP assay of the interaction of SDEL1/2 and SPX4 *in vivo*. Protein extracts (Input) were immunoprecipitated with anti-FLAG magnetic beads (IP; Sigma-Aldrich). Immunoblots were developed with an anti-FLAG antibody (Sigma-Aldrich) to detect SPX4 and with anti-GFP (Sigma-Aldrich) to detect SDEL1 and SDEL2. Molecular mass markers are shown (kDa).

(E) E3 Ub ligase activity was tested using various doses of His-tagged SDEL1 in the presence or absence of E1 and E2. An anti-His antibody was used to detect SDEL1 and ubiquitinated SDEL1 proteins (top). Anti-biotin antibody was used to detect ubiquitinated proteins (bottom) (ubiquitin was crosslinked with biotin).

(F) SDEL1 was able to ubiquitinate SPX4. Anti-GST and anti-biotin antibodies were used to detect ubiquitinated SPX4 proteins. Molecular mass markers are shown (kDa).

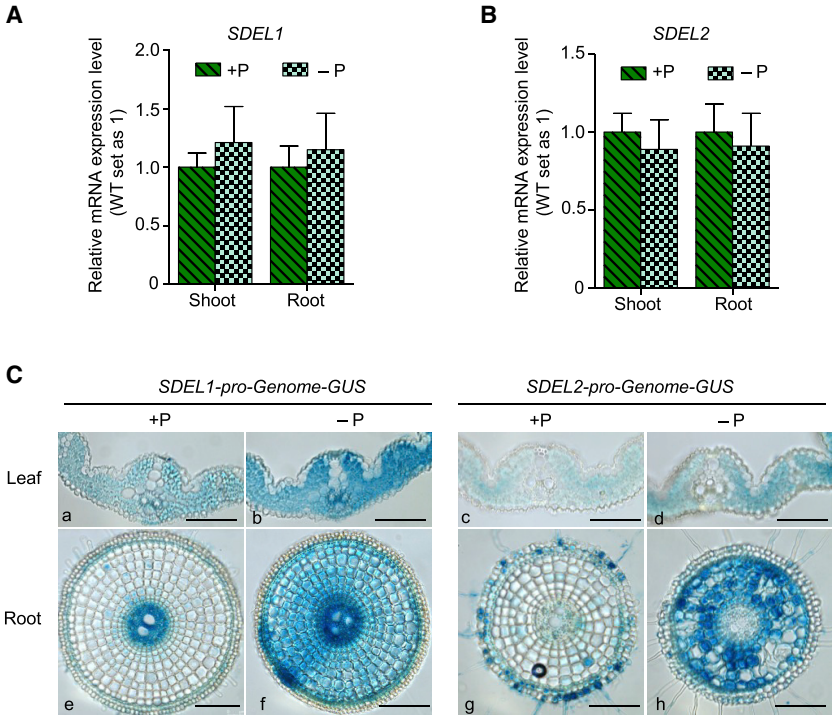

Figure 2. Pi-Deficiency Induces SDEL1 and SDEL2 Protein Accumulation.

(A and B) Relative expression levels of *SDEL1* **(A)** and *SDEL2* **(B)** under +P and −P conditions. The 14-day-old seedlings (wild type) grown under Pi-sufficient (200 μM) conditions were transferred into +P (200 μM Pi) or −P (0 μM Pi) solution and cultured for another 7 days before harvesting for RNA extraction. The mRNA expression levels of *SDEL1* and *SDEL2* were detected by qRT–PCR using specific primers for *SDEL1* and *SDEL2* (Supplemental Table 2). Values represent means ± SD of three replicates.

(C) GUS-staining analysis of *SDEL1pro-gSDEL1-GUS* and *SDEL2pro-gSDEL2-GUS* transgenic plants grown under +P (200 μM Pi) and −P (0 μM Pi). a and b, GUS staining of a leaf blade; c and d, GUS staining of a primary root. Scale bars, 100 μm.

SPX4, as revealed by the Rice Expression Database and β-glucuronidase (GUS) histochemical analysis of *SDEL1pro-gSDEL1-GUS* and *SDEL2pro-gSDEL2-GUS* plants (Figure 2 and Supplemental Figure 2). qRT–PCR analysis showed that the transcript levels of *SDEL1* and *SDEL2* were not responsive to Pi starvation. However, the protein levels of SDEL1 and SDEL2 were obviously induced under Pi-deficient conditions based on the GUS-activity analysis of the transgenic lines harboring the genomic *SDEL1* or *SDEL2* sequence fused with *GUS* (Figure 2).

To verify the initial library screening, we used SPX4 as bait to test the interaction with SDEL1. Y2H assays showed that SPX4 could interact with SDEL1 in yeast cells (Figure 1B). Given that Os03g22680 (SDEL2) is phylogenetically the most closely related protein to SDEL1 and is expressed in a similar pattern as SDEL1, we also chose it to test the interaction with SPX4 in yeast. Like SDEL1, SDEL2 also interacts with SPX4 in yeast cells (Figure 1B). To further validate the Y2H results, we conducted bimolecular fluorescence complementation (BiFC) assays in tobacco (*Nicotiana benthamiana*) leaves. SDEL1 and SDEL2 were located in the nucleus and the cytoplasm, the same localization pattern as that of SPX4 (Supplemental Figure 3; Lv et al., 2014). The co-expression of SDEL1-YFP^N/SPX4-YFP^C or SDEL2-YFP^N/SPX4-YFP^C led to a fluorescence signal in the nucleus and cytoplasm, as was observed for SPX4-YFP^N/SPX4-YFP^C (Lv et al., 2014), while co-expression of SDEL1-YFP^N/YFP^C and SDEL2-YFP^N/YFP^C did not produce any detectable fluorescence signal (Figure 1C). To further confirm that SDEL1 and SDEL2 actually interact with SPX4 *in planta*, we performed co-immunoprecipitation (co-IP) assays in tobacco leaves co-transformed with SPX4-FLAG/SDEL1-GFP or SPX4-FLAG/SDEL2-GFP. We found that both SDEL1 and SDEL2 interacted with SPX4 but not with the GFP control (Figure 1D). It is noteworthy that two specific bands for SPX4-FLAG could be detected in tobacco. Since the lower band was close to the predicted molecular weight of SPX4-FLAG, this indicates that there is some unknown modification of SPX4 *in planta*. Furthermore, two bands were also detected for SDEL2-GFP in the co-IP assays, which were both smaller than the predicted molecular weight of SDEL2-GFP. This indicates that SDEL2-GFP is not stable *in planta*. Together, these results show that the putative E3 ligases SDEL1 and SDEL2 physically interact with SPX4 *in vitro* and *in vivo*.

Since SDEL1 and SDEL2 contain the typical E3 ligase domain (Stone et al., 2005), we hypothesized that SDEL1 and SDEL2 have E3 ligase activity. To test this hypothesis, we attempted to express and purify His-tagged SDEL1 and SDEL2 in *Escherichia coli* (Supplemental Figure 4). However, only His-tagged SDEL1 (SDEL1-His) was successfully expressed and purified. We further performed *in vitro* ubiquitination assays using a commercial human E1 (E1-his, His-tagged) and E2 (UbcH5a-His), and His-tagged SDEL1 fusion proteins. As expected, the E2 protein was ubiquitinated in the presence of the E1 (Figure 1E, lane 1). When SDEL1 was added to the reaction, a protein ladder was detected using anti-biotin antibody (ubiquitin was crosslinked with biotin). This infers that SDEL1 has E3 Ub ligase activity. The E3 Ub ligase activity of SDEL1 was dependent on the presence of E1 and E2 and enhanced with increasing SDEL1 protein levels (Figure 1E, lanes 2–5).

We further tested whether SPX4 is a ubiquitination substrate of SDEL1. Incubation of glutathione *S*-transferase (GST)-tagged SPX4 with E1, E2, and SDEL1 led to the detection of a strong protein ladder signal (Figure 1F, lane 5), whereas incubation with E1 and E2 alone did not result in the addition of ubiquitin to SPX4 (Figure 1F, lane 4). This indicates that SDEL1 mediates SPX4 ubiquitination. Taken together, these results show that SDEL1 and SDEL2 can interact with SPX4 *in vitro* and *in vivo*, and that SDEL1 is a functional E3 Ub ligase able to ubiquitinate SPX4 *in vitro*.

SDEL1 and SDEL2 Are Responsible for SPX4 Stability

Given that SDEL1 and SDEL2 interact with and ubiquitinate SPX4 *in vitro*, we hypothesized that the ubiquitination and degradation of SPX4 *in vivo* is dependent on SDEL1 and SDEL2. To test this hypothesis, we generated *SDEL1* and *SDEL2* loss-of-function mutants and overexpressing lines (Supplemental Figures 5 and 7). CRISPR/Cas9 was used to generate loss-of-function mutants. Four and five independent successfully edited mutant lines with similar phenotypes (described later) were obtained for SDEL1 and SDEL2, respectively (Supplemental Figures 5 and 6). The *sdel1-1* and *sdel2-1* mutants were chosen for further analysis and crossed to generate the double mutant *sdel1-1 sdel2-1*. Cell-free degradation analysis of the recombinant GST-SPX4 protein in the total protein extracts from plants grown under Pi-deficient conditions was undertaken. The western blot results showed that GST-SPX4 was degraded with a half-life of ~6 min when incubated with the total protein extracts from wild-type (WT) or the *sdel2-1* mutant (Figure 3A and 3B). However, when incubated with the extracts from the *sdel1-1* mutant, the degradation half-life of GST-SPX4 was obviously longer than that in WT extracts. When incubated with the extract from the *sdel1-1/sdel2-1* double mutant, the degradation half-life was almost 2.5-fold that of GST-SPX4 incubated with WT extract. In contrast to the WT and mutant extracts, incubation with extracts from the *SDEL1* or *SDEL2* overexpression lines significantly shortened the degradation half-life of GST-SPX4 (Figure 3A and 3B). These results suggest that both SDEL1 and SDEL2 positively regulate the degradation of SPX4.

Given that SDEL1 and SDEL2 can ubiquitinate SPX4 to regulate its degradation, we hypothesized that the SPX4 protein levels are affected by SDEL1 and SDEL2 *in planta*. To test this we generated *35S-SPX4-FLAG* (hereafter *SPX4-FLAG*) transgenic rice plants (Supplemental Figure 8A and 8B). Consistent with a previous report (Lv et al., 2014), *SPX4-FLAG* plants displayed a lower Pi content as is seen in *SPX4* overexpressing lines, suggesting that the SPX4-FLAG fusion protein is functional *in vivo* (Supplemental Figure 8C). A stable *SPX4-FLAG* (*SPX4-FLAG-5*) transgenic line was chosen to develop *sdel1sdel2* double mutants using CRISPR/Cas9, and *SDEL1*- and *SDEL2*-overexpressing lines (*SDEL1-OE* and *SDEL2-OE*) (Supplemental Figure 9). The SPX4-FLAG protein levels in the WT, *sdel1sdel2*, *SDEL1-OE*, and *SDEL2-OE* genetic backgrounds were further analyzed by western blot with an anti-FLAG antibody. This analysis showed that the protein levels of SPX4 in the *sdel1sdel2* double mutant were obviously increased compared with those in the WT under both +P and −P conditions (Figure 3C). By contrast, in the *SDEL1-OE* and *SDEL2-OE* lines, the protein levels of SPX4 were much lower than those in WT under Pi-sufficient conditions (Figure 3C). These results suggest that SDEL1 and SDEL2 regulate SPX4 protein abundance by mediating its degradation.

Since SDEL1 ubiquitinated SPX4 *in vitro* and SPX4 was significantly degraded under −P conditions, we speculated that the extent of ubiquitination of SPX4 should be decreased in *sdel1sdel2* and increased in the *SDEL1*- and *SDEL2*-overexpressing lines under −P conditions *in planta*. To test this hypothesis, we grew 14-day-old seedlings of *SPX4-FLAG/WT*, *SPX4-FLAG/sdel1sdel2*, *SPX4-FLAG/SDEL1-OE*, and *SPX4-FLAG/SDEL2-OE* under −P conditions for 7 days. Plants were then transferred into −P solution supplemented with 20 μM MG132 (a proteasome inhibitor, which can block the degradation of ubiquitinated proteins) and cultured for another 2 days before harvesting for protein extraction. The SPX4 proteins, both ubiquitinated and non-ubiquitinated, were immunoprecipitated with anti-FLAG magnetic beads. SPX4 and ubiquitinated SPX4 were detected by immunoblotting with an anti-FLAG antibody and anti-Ubi antibody, respectively. In the presence of MG132 there were no obvious differences in SPX4 protein levels among WT, *sdel1sdel2*, and *SDEL*-overexpressing lines (Figure 3D). However, the level of polyubiquitinated SPX4 in the *sdel1sdel2* double mutant was significantly lower than that in WT, while the levels of polyubiquitinated SPX4 in *SDEL1*- and *SDEL2*-overexpressing lines were higher than those in the other genetic backgrounds (Figure 3D), suggesting that SDEL1 and SDEL2 are crucial for SPX4 ubiquitination in the plant. The above results together indicate that Pi-deficiency-induced SPX4 degradation is dependent on SDEL1 and SDEL2.

Lysine Residues K^{213} and K^{299} of SPX4 Are the Primary Ubiquitination Sites for SPX4

Given that SDEL1 and SDEL2 directly interact with SPX4 and ubiquitinate it both *in vitro* and *in vivo*, we further investigated the basis for the interaction of SDEL1 and SPX4. Using a Y2H assay, we showed that yeast cells co-transformed with the SPX domain of SPX4 ($SPX4^{1–208}$) and SDEL1 grew as well as those transformed with SPX4/SDEL1 did on SD/-LTH selection medium. This indicates that SDEL1 interacts with the SPX domain of SPX4. The SPX domain contains six α helices (Wild et al., 2016). Further analysis showed that the 159^{th} to 208^{th} amino acid residues of SPX4, which contain the fifth and sixth α helices, are essential for SPX4 and SDEL1 interaction (Figure 4A).

We further analyzed the possible ubiquitination sites of SPX4. Twenty-two lysine residues are present in SPX4, 18 of which are located in the SPX domain with the other four located in the C-terminus of SPX4 (Figure 4B). To narrow down the possible ubiquitination sites of SPX4, we checked the stabilities of truncated SPX4s in the total protein extracts of WT plants grown under −P conditions. We found that the SPX domain of SPX4 fused with GST (SPX4-N) was very stable, while the C-terminal part of $SPX4^{159–320}$ fused with GST (SPX4-C) was rapidly degraded in total protein extracts (Figure 4C). This indicated that the C-terminal part of SPX4 might be the target of ubiquitination. Further UbPred (Predictor of Protein Ubiquitination Sites) analysis of the C-terminal part of SPX4 indicated that K^{213} and K^{299} were the most likely ubiquitination sites (Supplemental Table 1). To determine whether SDEL1 could catalyze ubiquitination of these sites, we performed *in vitro* ubiquitination assays using WT and mutated versions of SPX4-C. As observed for the positive control, full-length SPX4, SPX4-C could be ubiquitinated by SDEL1 (Figure 4E, lanes 3 and 5). However, when the lysine residue K^{213} was mutated to arginine (R^{213}), which cannot be ubiquitinated and has a positive charge like lysine, the degree of SPX4-C^{K213R} ubiquitination was significantly decreased compared with that of SPX4-C (Figure 4E, lanes 5 and 6). Ubiquitination was negligible when both K^{213} and K^{299} were mutated to arginine (SPX4-$C^{K213R/K299R}$) (Figure 4E, lanes 2 and 7). These results demonstrate that SDEL1 can ubiquitinate the K^{213} and K^{299} residues of SPX4.

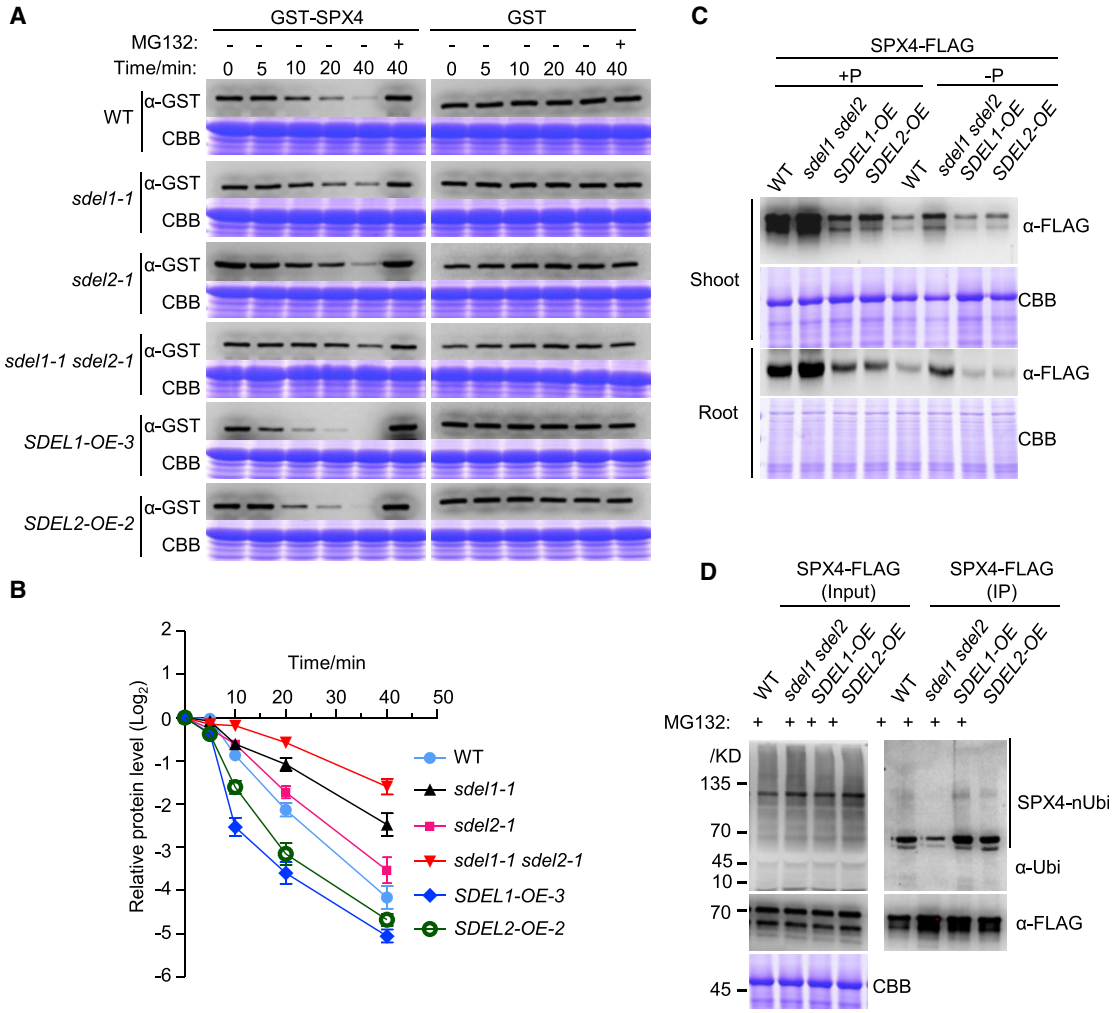

Figure 3. SDEL1 and SDEL2 Are Critical for the Degradation of SPX4.

(A) Cell-free degradation assay of SPX4 in wild type (WT), *sdel1-1*, *sdel2-1*, *sdel1-1 sdel2-1*, *SDEL1-OE-3*, and *SDEL2-OE-2*. GST fusions of SPX4 derivatives were expressed in *E. coli* and purified; 100 ng of each was incubated for different times at 28°C with protein extracts from leaves (20 mg total protein) of WT, *sdel1-1*, *sdel2-1*, *sdel1-1 sdel2-1*, *SDEL1-OE-3*, and *SDEL2-OE-2* rice plants cultured hydroponically under Pi deficiency for 7 days. The reaction was carried out without (−) or with (+) 40 μM MG132. GST-SPX4 and GST proteins were detected by western blotting using anti-GST antibody.

(B) The relative amount of GST-SPX4 remaining after incubation in different plant extracts was calculated and plotted on a log graph. The protein level of GST-SPX4 was normalized to that of a GST control. Data represent means ± SD (n = 3, three repeats of an individual incubation analysis).

(C) SPX4 levels in WT, *sdel1sdel2*, and the *SDEL1* and *SDEL2* overexpression lines. Proteins in shoots (upper panel) and roots (lower panel) of 21-day-old plants (*SPX4-FLAG*, *sdel1sdel2/SPX4-FLAG*, *SDEL1-OE/SPX4-FLAG*, *SDEL2-OE/SPX4-FLAG*) grown under +P and −P conditions were detected by immunoblot using an anti-FLAG antibody. Equal amounts of protein (100 μg) were used for immunoblotting. Coomassie brilliant blue (CBB) staining indicates similar amounts of proteins were loaded.

(D) Ubiquitination of SPX4 is mostly dependent on SDELs. Fourteen-day-old plants of *SPX4-FLAG*, *sdel1sdel2/SPX4-FLAG*, *SDEL1-OE/SPX4-FLAG*, and *SDEL2-OE/SPX4-FLAG* were transferred into −P solution for another 7 days; thereafter, 20 μM MG132 was added into the −P solution for another 2 days. Protein extracts (Input) were immunoprecipitated with anti-FLAG magnetic beads (IP). Immunoblots were performed with anti-FLAG antibody to detect SPX4, and with anti-Ub to detect ubiquitinated proteins. Coomassie brilliant blue (CBB) staining indicates that similar amounts of proteins were loaded. Molecular mass markers are shown (kDa).

Given that the K^{213} and K^{299} of SPX4 can be ubiquitinated by SDEL1, we hypothesized that K^{213} and K^{299} are the key sites responsible for the stability of SPX4. To test this hypothesis, we conducted cell-free degradation assays of GST-SPX4-$C^{K213R/K299R}$ and GST-$SPX4^{K213R/K299R}$ by incubating the recombinant proteins with total protein extracts from WT shoots grown under −P conditions. Western blot results showed that the degradation half-life of SPX4-C was similar to that of SPX4 (Figure 4C) , wheras the degradation half-life of GST-SPX4-$C^{K213R/K299R}$ and GST-$SPX4^{K213R/K299R}$ were significantly longer than those of SPX4-C and SPX4 (Figure 4C), indicating that K^{213} and K^{299} are crucial for SPX4 degradation. Together, these results suggest that SDEL1 interacts with the fifth and sixth α helix of the SPX domain to ubiquitinate K^{213} and K^{299} and mediate SPX4 degradation.

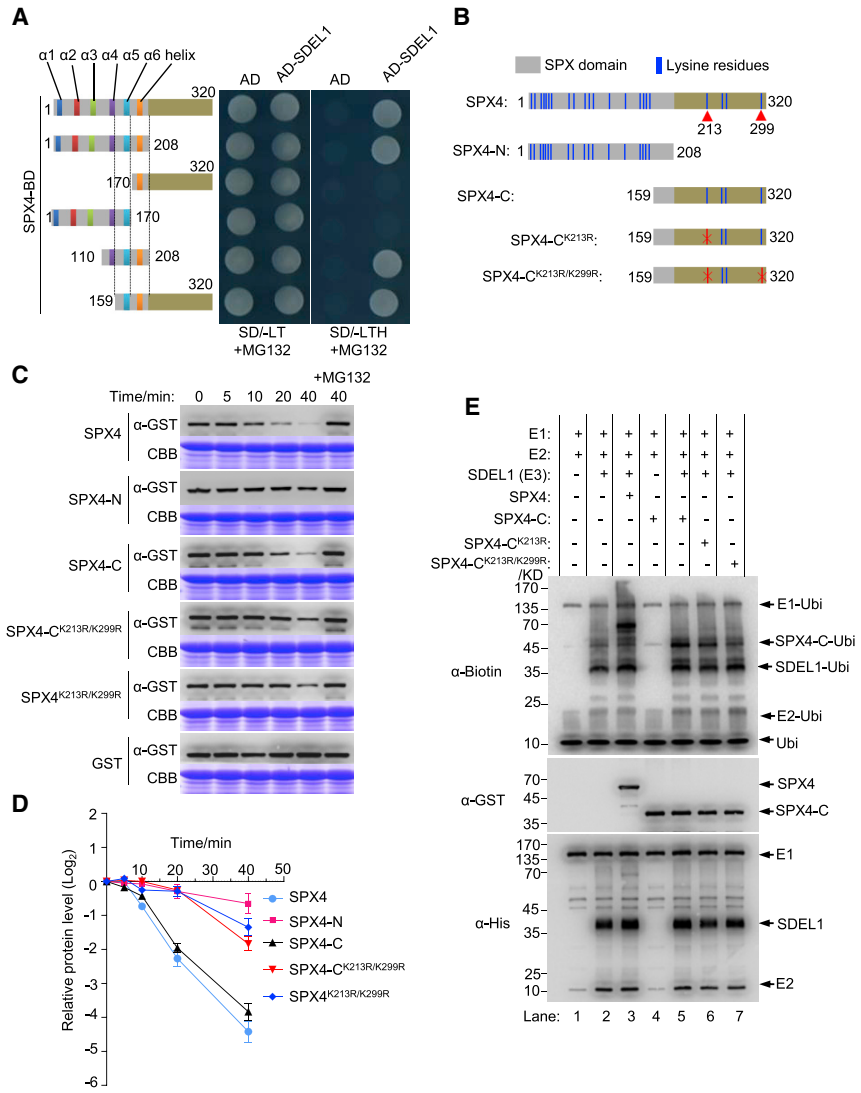

Figure 4. Lysine Residues K^{213} and K^{299} Are the Key Ubiquitination Sites of SPX4.

(A) Y2H assay showing the interaction of different truncates of SPX4 and SDEL1. Yeast cells co-transformed with BD-SPX4/AD-SDEL1, BD-$SPX4^{1–208}$/AD-SDEL1, BD-$SPX4^{170–320}$/AD-SDEL1, BD-$SPX4^{1–170}$/AD-SDEL1, BD-$SPX4^{110–208}$/AD-SDEL1, or BD-$SPX4^{159–320}$/AD-SDEL1 were grown on selective media (SD/-LT and SD/-LTH, plus 10 μM MG132 to avoid target protein degradation).

(B) Diagram of the SPX4 protein and different truncates. Gray box, the SPX domain of SPX4; blue lines, the lysine residues of SPX4; red arrows, the candidate ubiquitination sites; red lines, the relative positions of the mutated lysine residues. SPX4-N, the N-terminus of SPX4 from amino acids 1 to 208; SPX4-C, the C-terminus of SPX4 from amino acids 159 to 320; SPX4-C^{K213R}, lysine residue 213 was mutated to arginine; SPX4-$C^{K213R/K299R}$, the lysine residues 213 and 299 were mutated to arginine.

(C) Cell-free degradation assay of SPX4 and different truncated or mutated versions of SPX4. GST, GST-tagged SPX4, and different truncated or mutated versions of GST-tagged SPX4 (100 ng each) were incubated for different amounts of time at 28°C with protein extracts from wild-type leaves (20 mg of total protein). The reaction was carried out without (–) or with (+) 40 μM MG132. GST-SPX4 and GST proteins were detected by western blotting using anti-GST antibody. Coomassie brilliant blue (CBB) staining indicates that similar amounts of proteins were loaded.

(D) The relative amount of GST-SPX4 remaining after incubation in wild-type extracts was calculated and plotted on a log graph. The protein levels of SPX4, SPX4-N, SPX4-C, SPX4-C^{K213R}, and SPX4-$C^{K213R/K299R}$ were normalized to those of a GST control. Data represent means ± SD (n = 3, three repeats of an individual incubation analysis).

(E) Ubiquitination assay of SPX4 and different truncated or mutated versions of SPX4. Anti-biotin antibody was used to detect ubiquitinated proteins; anti-GST antibody was used to detect full-length and truncated or mutated versions of GST-tagged SPX4; anti-His antibody was used to detect His-tagged SDEL1, E1, and E2. Molecular mass markers are shown (kDa).

SPX4–PHR2 Complex Formation Prevents Ubiquitination by SDELs

It has been reported that SPX4 interacts with PHR2, a central regulator of Pi signaling, in the presence of IPs (such as IP_6) (Wild et al., 2016). We hypothesized that interaction with PHR2 can protect SPX4 from ubiquitination by SDEL1 and SDEL2 and retard its degradation. To test this hypothesis, we performed *in vitro* ubiquitination assays. The results showed that PHR2 cannot be ubiquitinated by SDEL1; the ubiquitination signals detected from the reaction of PHR2/SDEL1/E2/E1 were comparable with those from the reaction of SDEL1/E2/E1 (Figure 5A, lanes 2, 3, and 4). Furthermore, the addition of IP_6 (20 μM) had no effect on the ubiquitination of SPX4 by SDEL1 (Figure 5A, lanes 4 and 5). However, in the presence of IP_6, the addition of PHR2 reduced the ubiquitination of SPX4 in a dose-dependent manner (Figure 5A, lanes 5 and 6), while without IP_6 the efficiency with which PHR2 blocked the ubiquitination of SPX4 was significantly reduced (Supplemental Figure 11, lanes 7 and 8). These results demonstrate that interaction with PHR2 could prevent the ubiquitination of SPX4 by SDEL1 and SDEL2 and that this process is dependent on the presence of IPs.

To further confirm that PHR2 protects SPX4 from degradation, we performed cell-free degradation assays of SPX4 by incubating GST-SPX4 with total protein extracts from WT, a *PHR2*-overexpressing line (*PHR2-OE*) (Zhou et al., 2008) and the *phr1phr2* double mutant (Guo et al., 2015) grown under Pi-sufficient conditions. The degradation half-life of GST-SPX4 in the *PHR2-OE* extract was about 20 min, which is significantly longer than that in the WT extract (about 15 min) (Figures 5B and 5C). By contrast, the degradation half-life of GST-SPX4 in the *phr1phr2* double mutant extract (less than 10 min) was obviously shorter than that in the other extracts (Figure 5B and 5C). These results indicate that PHR2 could protect SPX4 from degradation under Pi-sufficient conditions.

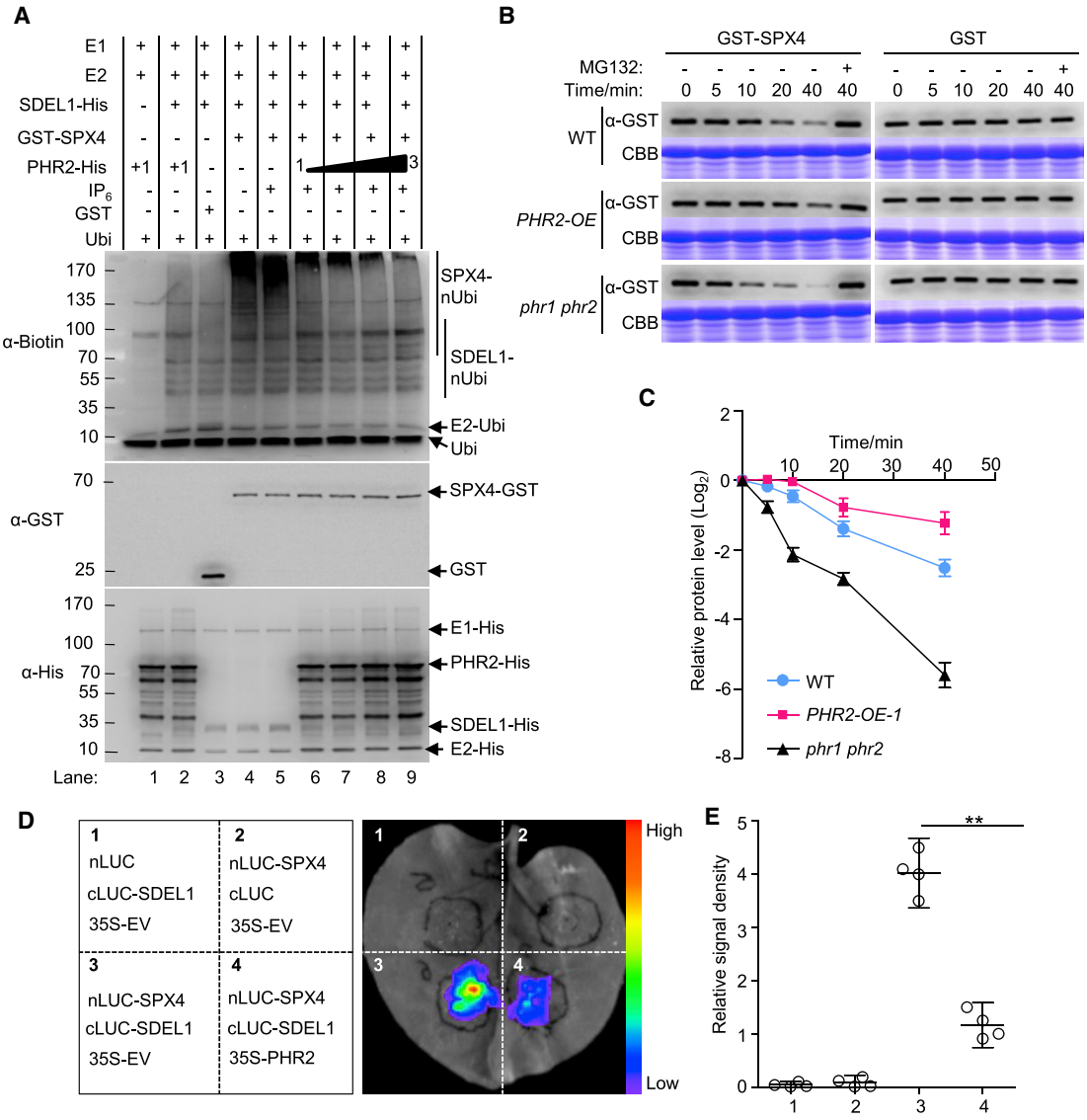

Figure 5. PHR2 Competes with SDEL1 to Interact with SPX4 and Prevents the Ubiquitination of SPX4.

(A) PHR2 prevents SDEL1 from ubiquitinating SPX4 *in vitro*. GST-tagged SPX4 and His-tagged SDEL1 PHR2 were expressed in *E. coli* and purified. The ubiquitination level of SPX4 was assayed in the absence or presence of different concentrations of PHR2. IP_6 is an inositol hexaphosphoric acid that stabilizes the interaction between PHR2 and SPX4. Anti-biotin antibody was used to detect ubiquitinated proteins; anti-GST antibody was used to detect full-length and truncated or mutated versions of GST-tagged SPX4; anti-His antibody was used to detect His-tagged SEDL1, PHR2, E1, and E2. Molecular mass markers are indicated (kDa).

(B) Cell-free degradation assay of SPX4 in wild type (WT), *PHR2-OE-1*, and *phr1phr2* extracts. One hundred nanograms of SPX4-GST or GST were incubated for different times at 28°C with protein extracts from leaves (20 mg of total protein) of WT, *PHR2-OE-1*, and *phr1phr2* grown under +P conditions. The reaction was carried out without (−) or with (+) 40 μM MG132. GST-SPX4 and GST proteins were detected by western blotting using an anti-GST antibody. Coomassie brilliant blue (CBB) staining indicates that similar amounts of proteins were loaded.

(C) The relative amounts of GST-SPX4 remaining after incubation in wild-type (WT), *PHR2-OE-1*, and *phr1phr2* extracts were calculated and plotted on a log graph. The protein level of GST-SPX4 was normalized with that of a GST control. Data represent means ± SD (n = 3, three times individual incubation analysis).

(D) PHR2 competes with SDEL1 to interact with SPX4. LCI assays for detecting protein interactions were performed in tobacco leaves. The vector combinations nLUC/cLUC-SDEL1/35S-EV and nLUC-SPX4/cLUC/35S-EV were used as negative controls; nLUC-SPX4/cLUC-SDEL1/35S-EV was used to test the interaction density between SPX4 and SDEL1; nLUC-SPX4/cLUC-SDEL1/35S-PHR2 was used to test the competition between SDEL1 and PHR2 for interaction with SPX4. The vectors were co-infiltrated into tobacco leaves, and the LUC activities were analyzed 48 h after infiltration. EV indicates the empty vector used to construct *35S-PHR2*.

(E) Quantifications of the relative lunminescence intensities in **(D)** were plotted on a Log_{10} graph. Data represent means ± SD (n = 4, four repeats in different tobacco leaves in one experiment). (**p < 0.01; Student's t test).

Since both SDEL1 and PHR2 can interact with the SPX domain of SPX4 (Lv et al., 2014 and Figure 4A), we hypothesized that PHR2 can compete with SDELs to interact with SPX4, thus preventing SDELs from accessing SPX4. To test this hypothesis, we performed luciferase (LUC) complementation imaging (LCI) assays in tobacco leaves. Consistent with the interaction between SPX4 and SDEL1, a strong firefly luciferase activity signal was detected in the leaves co-transformed with nLUC-SPX4/cLUC-SDEL1/35S-EV (Figure 5D and 5E). However, when 35S-PHR2 was co-transformed with nLUC-SPX4/cLUC-SDEL1, the signal was significantly decreased (Figure 5D and 5E). This indicates that PHR2 could compete with SDEL1 to form a complex with SPX4 *in planta*.

SDEL1 and SDEL2 Positively Regulate Pi Accumulation and Pi Signaling in Rice

Given that SPX4 is a key negative regulator of Pi homeostasis and Pi signaling (Lv et al., 2014), and that SDEL1 and SDEL2 directly regulate the degradation of SPX4, we hypothesized that SDEL1 and SDEL2 play a positive role in regulating Pi homeostasis and Pi signaling. To test this hypothesis, we analyzed the phenotype of *SDEL*-overexpressing lines (Figure 6A and Supplemental Figure 11A). Consistent with our hypothesis, the shoot and root Pi concentrations of the *SDEL1*- and *SDEL2*-overexpressing lines were obviously increased compared with those of WT grown under Pi-sufficient conditions (200 μM Pi) (Figure 6D). Under Pi-deficient conditions (10 μM Pi), the Pi concentration in the shoot of *SDEL*-overexpressing lines remained obviously higher than that of WT (Supplemental Figure 11D). The dry weights of *SDEL*-overexpressing lines were also lower than those of WT (Figure 6C and Supplemental Figure 11C).

We further analyzed Pi signaling by evaluating the expression levels of phosphate starvation-induced (*PSI*) genes (*IPS1*, *miR827*, *SPX1*, and *PT10*) in *SDEL1*- and *SDEL2*-overexpressing lines grown under Pi-sufficient conditions. We found that the expression levels of these *PSI* genes in *SDEL1*- and *SDEL2*-overexpressing lines were significantly induced compared with those in WT (Figure 6E).

Given that *SDEL1*- and *SDEL2*-overexpressing lines exhibit a Pi overaccumulation phenotype and show Pi-starvation signaling even under Pi-sufficient conditions, we hypothesized that the loss-of-function mutants of *SDEL1* and *SDEL2* would have reduced Pi contents and inhibited Pi signaling. We analyzed the phenotype and Pi concentration of *sdel1-1* and *sdel2-1* mutants and found that the biomass of *sdel1-1* and *sdel2-1* mutants were significantly lower than those of WT (Figure 6C and Supplemental Figure 11C), suggesting that *SDEL1* and *SDEL2* are crucial for plant growth. Pi-content analysis showed that the Pi concentrations of the *sdel1-1* mutant were obviously decreased compared with those of WT under Pi-sufficient conditions, while there were no significant differences between the *sdel2-1* mutant and WT (Figure 6D). Further analysis of *PSI* gene (*IPS1*, *miR827*, *SPX1*, and *PT10*) expression in the *sdel1-1* and *sdel2-1* mutants under Pi-deficient conditions showed that Pi signaling was significantly inhibited in the *sdel1-1* mutant, but similar to that in WT in the *sdel2-1* mutant (Figure 6F). The reduction in biomass, Pi concentration, and Pi signaling was further enhanced in the *sdel1-1 sdel2-1* double mutant (Figure 6C and 6D; Supplemental Figure 11C), suggesting functional redundancy between *SDEL1* and *SDEL2*. Further temporal response analysis of *PSI* gene expression showed that the induction of *PSI* gene expression by the Pi starvation in the double-mutant background was much slower than that in WT, which was comparable with that in the *SPX4* overexpression line (Supplemental Figure 12). These results indicate that SDEL1 and SDEL2 are crucial for plant growth and positively regulate Pi accumulation and Pi signaling in rice.

DISCUSSION

Pi is an essential macronutrient element for plant growth and development and is also an important signaling molecule Our understanding of the regulatory network for Pi sensing and signaling in plants is emerging. SPX proteins, which mediate the regulation of Pi-starvation signaling and Pi homeostasis in plants, are important regulators in this network (Secco et al., 2012a; Jung et al., 2018). Despite the accumulation of knowledge of the functional diversities of SPXs and the regulation of their transcription, how the stability of SPXs is regulated in response to the external Pi availability remains obscure.

Here we provide multiple lines of evidence supporting that rice SDEL1 and SDEL2 act as ubiquitin E3 ligases and promote SPX4 degradation. SDEL1 and SDEL2 are CHY zinc-finger and RING-finger domain-containing E3 ligases (Figure 1A). These E3 ligases are widely present in eukaryotes, and have divergent functions in plants. In *Arabidopsis*, a few CHY zinc-finger and RING-finger domain-containing E3 ligases have been characterized. It has been reported that CHYR1 (CHY ZINC-FINGER AND RING PROTEIN 1) mediates stomatal movement and drought tolerance (Ding et al., 2015). Nucleus-located MIEL1 (MYB30 INTERACTING E3 LIGASE 1) interacts with and ubiquitinates MYB30 to regulate defense responses (Marino et al., 2013). The membrane-bound DNF (DAY NEUTRAL FLOWERING) regulates flowering time by repressing the expression of *CONSTANS* (*CO*) (Morris et al., 2010). BRUTUS negatively regulates the response to iron deficiency (Hindt et al., 2017). We showed that SDEL1 and SDEL2 are located in the nucleus and cytoplasm, function in regulating Pi signaling and Pi accumulation, and are crucial for plant growth in rice. It was reported that an *SPX4* loss-of-function mutant displayed upregulation of *PSI* genes even under Pi-sufficient conditions, and expression of *PSI* genes was repressed in SPX4 overexpression lines under Pi-deficient stress (Lv et al., 2014). Consistent with the role of SDELs in the degradation of SPX4, the expression of *PSI* genes under Pi-deficient stress in the *sdel1sdel2* double mutant was significantly repressed (Figure 6F), while *PSI* expression in the *SDEL1* and *SDEL2* overexpression plants was induced even under Pi-sufficient conditions (Figure 6E). Therefore, SDEL1 and SDEL2 are positive regulators of Pi accumulation and signaling.

SDEL1 could ubiquitinate SPX4 in the presence of E1 and E2 *in vitro* (Figure 1F). The SPX4 ubiquitination level was significantly decreased in the *sdel1sdel2* double mutant and increased in the *SDEL1*- and *SDEL2*-overexpressing lines (Figure 3D). Consistent with the role of SDEL1 and SDEL2 in SPX4 ubiquitination, the abundance of SPX4 protein was increased in the *sdel1sdel2* double-mutant background and

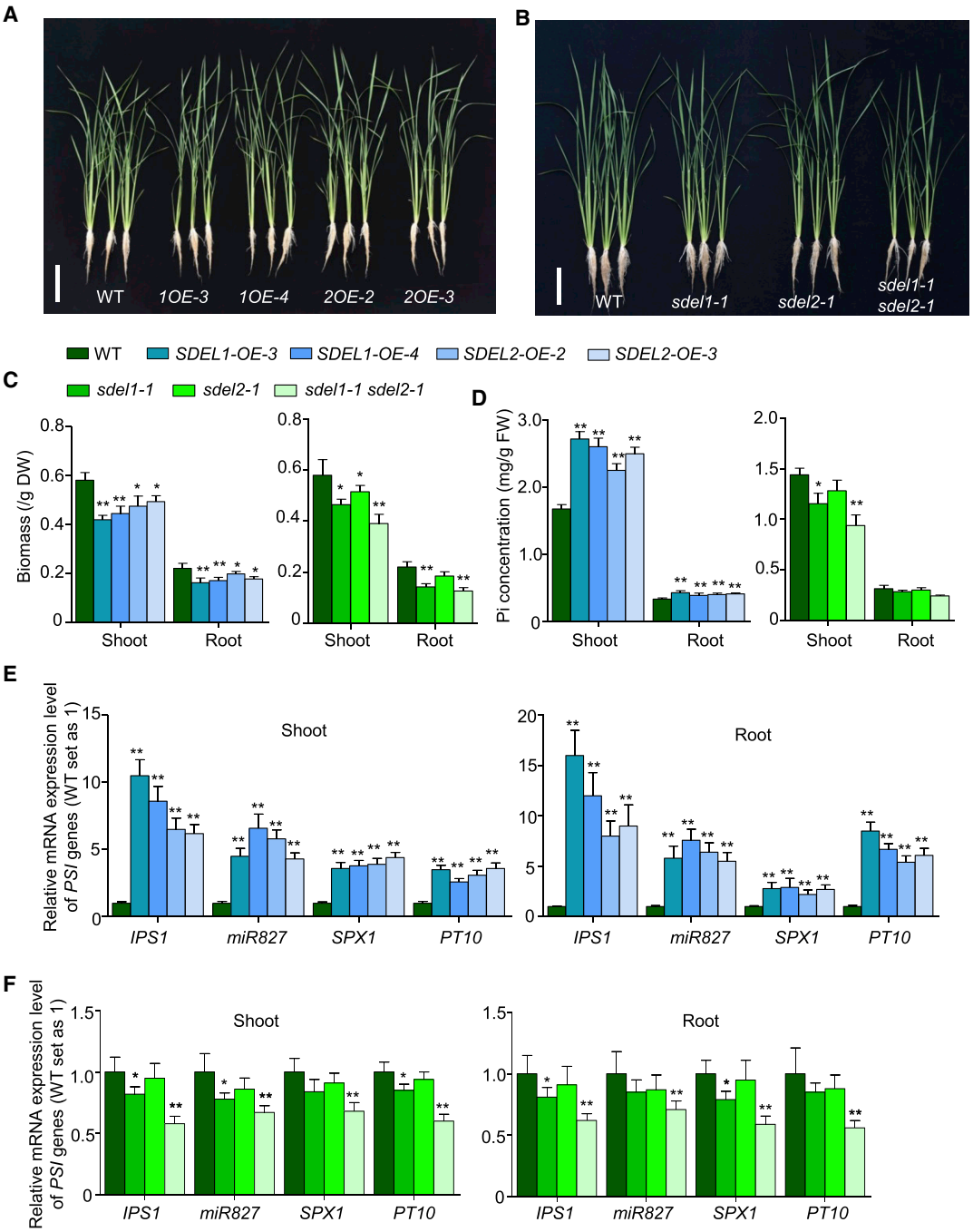

Figure 6. SDELs Regulate Both Pi Homeostasis and Pi Signaling.

(A and B) Phenotypic performance of 30-day-old wild type (WT), *SDEL1-OE-3* (*1OE-3*), *SDEL1-OE-4* (*1OE-4*), *SDEL2-OE-2* (*2OE-2*), and *SDEL2-OE-3* (*2OE-3*) **(A)**, and WT, *sdel1-1*, *sdel2-1*, and *sdel1-1 sdel2-1* **(B)**, under Pi-sufficient conditions. Scale bars, 10 cm.

(C and D) Bar graphs of dried biomass **(C)** and cellular Pi concentration **(D)** of shoots and roots of 30-day-old wild-type (WT) plants, *SDEL1-OE-3*, *SDEL1-OE-4*, *SDEL2-OE-2*, and *SDEL2-OE-3* overexpression lines, and *sdel1-1*, *sdel2-1*, and *sdel1-1 sdel2-1* mutants under Pi-sufficient conditions.

(E) Enhancing the expression of *SDEL1* and *SDEL2* induced Pi-starvation signaling under Pi-sufficient conditions. RNA was isolated separately from shoots and roots of 20-day-old plants grown in Pi-sufficient solution, and qRT–PCR was performed using specific primers (listed in Supplemental Table 2) for *IPS1*, *miR827*, *SPX1*, and *PT10*. Values represent means ± SD of three replicates.

(F) Mutation of SDEL1 and SDEL2 repressed Pi-starvation signaling. The 14-day-old plants of WT, *sdel1-1*, *sdel2-1*, and *sdel1-1 sdel2-1* were transferred into −P solution for another 7 days. The shoots and roots were harvested for RNA extraction and qRT–PCR analysis using specific primers for *IPS1*, *miR827*, *SPX1*, and *PT10* (listed in Supplemental Table 2).

Values represent means ± SD of three replicates. The expression level of WT was set as 1. The *P* values for comparisons with WT are indicated in **(C)** to **(F)** (* $P < 0.05$, ** $P < 0.01$; Student's *t*-test).

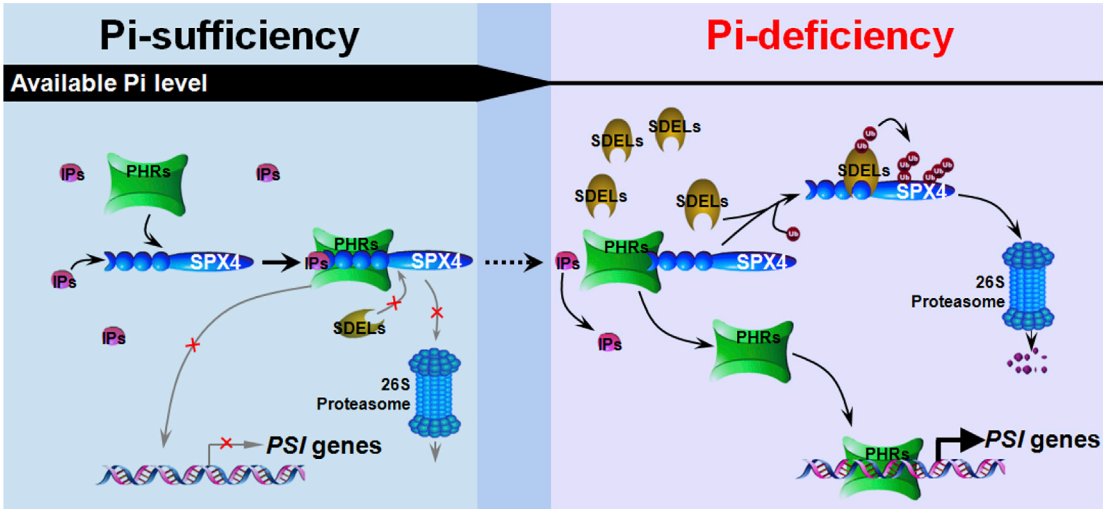

Figure 7. A Working Model of the SDEL–PHR–SPX Module in Regulating Pi-Deficiency Response.
The model illustrates how the Pi-signal regulators SDELs, SPX4, and PHRs co-regulate Pi-starvation response. Under Pi-sufficient conditions, the formation of SPX4-IPs-PHRs complex prevents the SPX4 degradation by SDELs, and inhibits the activation of downstream *PSI* genes. While, under Pi-deficiency, the accumulation of SDELs facilitates the degradation of SPX4, which is dissociated from PHRs due to the decreased IPs. Therefore, the PHRs can activate the downstream *PSI* genes. The red crosses indicate inhibition of a regulatory process. IPs, inositol pyrophosphates; Ub, ubiquitin; *PSI*, phosphate starvation-induced.

decreased in the *SDEL1*- and *SDEL2*-overexpressing lines. This indicates that SDEL1 and SDEL2 mediate the ubiquitination and proteasomal degradation of SPX4 in rice. Additionally, we noticed that even though the GST-SPX4 protein was much more stable in total protein extracts of the *sdel1sdel2* double mutant than in those of WT, the GST-SPX4 protein could still be degraded after further incubation (Figure 3A). This suggests that there are still other E3 ligases mediating the ubiquitination and stability of SPX4. Given the presence of *SDEL1* and *SDEL2* homologs in the rice genome, it is possible that these homologs also participate in SPX4 degradation (Supplemental Figure 1). Furthermore, we could not rule out that other E3 ligases also participate in the degradation of SPX4 *in planta*. Recently, it has been reported that a RING-H2-finger domain-containing E3 ligase, NBIP1, could regulate the stability of SPX4 in response to nitrate availability (Hu et al., 2019). Characterization of the coordination of the SDELs and NBIP1 for SPX4 degradation will help to further illustrate the crosstalk between nitrate and Pi signaling.

We also found that the SPX domain of SPX4 provides the platform for interaction with SDEL1 and SDEL2 (Figure 4). SPX domains have been reported to have important roles in protein interaction. For example, the SPX domain of NLA1 is responsible for its interaction with PHOSPHATE TRANSPORTERs (PTs), and PHO2, a ubiquitin-conjugating E2 enzyme (UBC24), interacts with the SPX domain of PHO1 (Liu et al., 2012; Lin et al., 2013; Yue et al., 2017). It has also been reported that several Lys and Tyr residues in the second and fourth α helices of the SPX domain contribute to the formation of a positively charged ligand-binding surface. IP_6 binding to this surface can promote the specific interaction of SPXs with other interacting proteins. For example, the presence of IP_6 in the SPX domain can facilitate the interaction between SPX4 and PHR2 (Wild et al., 2016). Although SDEL1 also interacts with the SPX domain of SPX4, we found that the ubiquitination of SPX4 by SDEL1 was not dependent on the presence of IP_6. This might be explained by the evidence that SDEL1 interacts with the fifth and sixth α helices of the SPX domain of SPX4 (Figure 4A). However, the interaction between SPX4 and PHR2 can prevent SDEL1 from accessing the fifth and sixth α helices of SPX4 (Figure 4A). Thus, the external Pi availability can favor the formation of different protein complexes. Under Pi-sufficient conditions, the presence of IP_6 could enhance the formation of the SPX4–PHR2 complex, which prevents SDEL1 and SDEL2 from accessing SPX4 and targeting it for degradation. Conversely, under Pi-deficient conditions the dissociation of the SPX4–PHR2 complex releases SPX4 to SDEL1 and SDEL2, leading to ubiquitination and proteasomal degradation. This is consistent with the evidence that the degradation half-life of SPX4 under Pi-deficient stress was faster than that under Pi-sufficient conditions (Lv et al., 2014). Furthermore, the degradation half-life of SPX4 was be prolonged and shortened in the PHR2-overexpressing lines and *phr1phr2* double-mutant background, respectively (Figure 5B).

We showed that K^{213} and K^{299} at the C terminus of SPX4 are the major ubiquitination sites responsible for its stability. Given that the C-terminal regions of the SPXs are the most variable, the divergence among them might affect their functions and protein properties. In line with this hypothesis, the subcellular localization patterns of the six SPXs in rice are different: OsSPX3/4/5/6 are located in the nucleus and cytoplasm, while OsSPX1/2 are exclusively located in the nucleus (Lv et al., 2014; Shi et al., 2014; Wang et al., 2014; Zhong et al., 2018). Furthermore, as all six rice SPXs have been confirmed to interact with PHR2, we speculate that other SPXs might also be protected by mechanisms similar to that of SPX4 in plants. In this regard, further work is still needed to unveil how the degradation of other SPXs is regulated.

We propose a working model illustrating how SDELs, SPX4, and PHRs coordinately regulate Pi signaling and Pi homeostasis in response to Pi availability in rice (Figure 7). Under Pi-sufficient conditions, SPX4 and PHRs form stable heterodimers with the help of IPs, which prevent SDELs from accessing SPX4 and thus prevent SPX4 degradation. Meanwhile, the formation of the SPX4–IPs–PHRs complex prevents PHRs from being targeted to the nucleus and efficiently activating downstream genes. However, under Pi-deficient stress, the IP content *in planta* is decreased, which leads to the dissociation of SPX4 from PHRs. The accumulation of SDELs facilitates the ubiquitination and degradation of the free SPX4 proteins, which further ensures the release of PHRs. Therefore, PHRs can efficiently enter the nucleus and bind to the promoters of the downstream PSI genes and quickly activate their expression, leading to Pi-starvation responses. Since the external Pi availability could be conveyed by the IPs in the cells, the SDELs, SPX4, and PHRs could form an indispensable network that integrates internal Pi status to modulate Pi signaling and homeostasis in rice. Understanding the mechanism by which the protein stability of SPX4 is regulated can enable us to breed smart crops better able to sense external and internal Pi availability, which might help to increase Pi efficiency in the field.

METHODS

Plant Materials and Growth Conditions

All rice (*Oryza sativa*) plants used in this study were derived from the *japonica* variety *Nipponbare*. The plants expressing *SPX4-FLAG* fusions were obtained by transforming *35S-SPX4-FLAG* into WT *Nipponbare*. The mutants *sdel1* and *sdel2* in the WT *Nipponbare* background and the double mutant *sdel1sdel2* in the *SPX4-FLAG* background were generated using the CRISPR/Cas9 technique (Mao et al., 2013). Four and five independent successfully edited mutation lines of *sdel1* and *sdel2* with similar phenotypes were obtained, respectively. The *sdel1-1* and *sdel2-1* mutants were chosen for further analysis. The double mutant *sdel1-1 sdel2-1* in the WT *Nipponbare* background were obtained by crossing *sdel1-1* and *sdel2-1*. One site in both *SDEL1* and *SDEL2* was targeted by CRISPR/Cas9 (The site in *SDEL1* is AAG ACG GCC ACG AGC TCG AT; the site in *SDEL2* is GAC GTG GGC AAG ATG GAG CA). The primers used to identify mutations in *SDEL1* and *SDEL2* are listed in Supplemental Table 2. Lines overexpressing *SDEL1* and *SDEL2* (both in the WT and *SPX4-FLAG* backgrounds) were obtained by transforming the *35S-SDEL1* or *35S-SDEL2* vector into callus.

The Pi-sufficient (+P) and Pi-deficient (−P) treatments were performed using normal rice culture solution (Yoshida et al., 1976) containing 200 and 0 mM Pi, respectively. The nutrient solution was adjusted to pH 5.5 using 1 M NaOH and replaced every 2 days during treatment. The experiments were performed in a greenhouse with a 12-h-day (30°C)/12-h-night (22°C) photoperiod, with a 200 μmol m^{-2} s^{-1} photon density and 60% humidity.

Construction of Plasmids and Generation of Transgenic Plant Lines

The *35S-SPX4-FLAG* vector was constructed by cloning the open reading frame of *SPX4* (Os03g61200) into a modified binary expression vector, *pF3PZPY122*, downstream of the cauliflower mosaic virus 35S promoter. To generate the vectors *35S-SDEL1* and *35S-SDEL2*, we cloned the open reading frame of *SDEL1* (Os12g35320) and *SDEL2* (Os03g22680) into a modified binary expression vector, *pCAMBIA1300*, downstream of the 35S promoter. The vectors *CRISPR-SDEL1*, *CRISPR-SDEL2*, and *CRISPR-SDEL1/SDEL2* were constructed according to the instructions of Ma et al. (2015). In brief, the target sequences of *SDEL1* and *SDEL2* were fused to the promoters of the rice RNA genes *U3* and *U6a*, respectively, then ligated into the binary vector *pYLCRISPR/Cas9-MT* (l). All constructs mentioned above were transformed into mature embryos from the seeds of *Nipponbare* or *SPX4-FLAG* via *Agrobacterium tumefaciens* (strain EHA105) as described previously (Hiei et al., 1994).

RNA Extraction, RT–PCR, and qPCR Assays

Total RNA from shoots and roots were extracted using the Plant RNA Extraction Kit (Promega) following the manufacturer's instructions. Reverse transcription was performed using a Moloney Murine Leukemia Virus Reverse Transcriptase cDNA Synthesis Kit (Promega) according to the manufacturer's instructions. qRT–PCR was performed as previously described (Zhou et al., 2008). The rice *Actin* (Os03g50890) gene was used as an internal control. Three biological replicates were performed per gene. Three technical replicates were performed per gene within an experiment.

Y2H Assays

The matchmaker GAL4 two-hybrid system (Clontech) was used for Y2H assays. The coding sequences (CDSs) of *SDEL1* and *SDEL2* were cloned into the *pGADT7* vector to generate *AD-SDEL1* and *AD-SDEL2*. The full-length and various truncates of SPX4 were cloned into the *pGBKT7* vector, generating *BD-SPX4*, *BD-SPX4*$^{1–208}$, *BD-SPX4*$^{170–320}$, *BD-SPX4*$^{1–170}$, *BD-SPX4*$^{110–208}$, and *BD-SPX4*$^{159–320}$. Related primers are listed in Supplemental Table 2. Different vector combinations were co-transformed into yeast (AH109). The selection medium used was SD/–T–L (without tryptophan and leucine, for selecting positive clones) and SD/-T-L-H (without tryptophan, leucine, and histidine, for selecting positive interaction clones). All media had 10 μM MG132 (*N*-benzyloxycarbonyl-L-leucyl-L-leucyl-L-leucinal) added to avoid degradation of target proteins in yeast cells as previously described (Ye et al., 2018).

BiFC Assays

The CDSs of *SDEL1*, *SDEL2*, and *SPX4* were cloned in frame with either the C-terminal or N-terminal fragments of YFP (Shen et al., 2011). Specific primers used are listed in Supplemental Table 2. The constructs were transiently expressed in *Nicotiana benthamiana* leaves by *Agrobacterium*-mediated infiltration (stain EHA105) as described previously (Walter et al., 2004). YFP fluorescence in *N. benthamiana* leaves was imaged at 2 days after infiltration using a Zeiss LSM710NLO confocal laser scanning microscope.

Co-immunoprecipitation Assays

The CDSs of *SDEL1* and *SDEL2* were cloned into the modified vector *pCAMBIA1300-GFP* to generate *35S-SDEL1-GFP* and *35S-SDEL2-GFP*. The CDS of *SPX4* was cloned into the modified vector *pF3PZPY122* to generate *35-SPX4-FLAG*. Different combinations of vectors were transiently expressed in *N. benthamiana* leaves using *Agrobacterium*. The co-immunoprecipitation assays were performed as described by Feng et al. (2008). The protein complexes were immunoprecipitated using anti-FLAG magnetic beads (Sigma-Aldrich) and detected with anti-GFP (Sigma-Aldrich) and anti-FLAG (Sigma-Aldrich) antibodies.

Subcellular Localization Analysis of SDEL1 and SDEL2 in Rice Protoplast Cells

Vectors containing *35S-SDEL1-GFP* and *35S-SDEL2-GFP* were transiently expressed in rice protoplast cells as described previously (Chen et al., 2011). Images were taken using a Zeiss Axiovert LSM 710 laser scanning microscope. GFP fluorescence was detected at 493–542 nm.

Cell-Free Degradation

The cell-free degradation assays were performed as previously described (Lv et al., 2014). In brief, the shoots of seedlings (WT, *sdel1*, *sdel2*, *sdel1sdel2*, *phr1phr2*, *SDEL1-OE*, and *SDEL2-OE*) grown under +P or −P conditions were harvested and frozen in liquid nitrogen for total protein

extraction. Total proteins were extracted in degradation buffer (25 mM Tris–HCl [pH 7.5], 10 mM NaCl, 10 mM $MgCl_2$, 4 mM phenylmethylsulfonyl fluoride [PMSF], 5 mM dithiothreitol, and 10 mM ATP) and adjusted to equal concentrations in degradation buffer for each assay. The purified proteins of GST, GST-SPX4, GST-SPX4-N, GST-SPX4-C, GST-SPX4-C^{K213R}, GST-SPX4-$C^{K213R/K299R}$, and GST-$SPX4^{K213R/K299R}$ were incubated with various protein extracts at 28°C for 0, 5, 10, 20, and 40 min. The GST-tagged proteins were detected by an anti-GST antibody (TransGen Biotech) diluted 1:5000. Quantitative analysis of immunoblots was performed using the Quantity Tools of Image Lab software (Bio-Rad).

Recombinant Protein Purification and *In Vitro* Ubiquitination Assays

SDEL1-His, PHR2-His, GST-SPX4, and SPX4-related truncates or mutated proteins were overexpressed and purified from *E. coli* BL21 (DE3) cell cultures using standard protocols. *In vitro* ubiquitination assays were performed using a Ubiquitinylation Kit (Enzo Life Sciences, BML-UW9920-0001) according to the manufacturer's instructions. The UBCH5a E2 enzyme in the kit was used in this study. Ubiquitin, conjugated to biotin, was detected by immunoblotting with stabilized streptavidin–horseradish peroxidase (HRP) conjugate.

Gel Blot Analysis

Antibodies used for western blotting were anti-GFP-HRP (G1544, Sigma, 1:5000), anti-FLAG-HRP (M2, Sigma, 1:5000), anti-His-HRP (Sigma, 1:5000), anti-GST-HRP (TransGen Biotech, 1:5000), mouse monoclonal anti-Ubi-HRP (Santa Cruz Biotechnology, 1:2000), goat anti-rabbit-IgG-HRP (Sigma, 1:10 000), and goat anti-mouse-IgG-HRP (Sigma, 1:10 000). Total plant proteins were extracted using extraction buffer (containing 25 mM Tris–HCl [pH 7.5], 10 mM NaCl, 4 mM PMSF, 20 μM MG132, and protease inhibitor cocktail). Proteins were visualized using the Immobilon kit (Millipore) under standard conditions. Quantitative analysis of immunoblots was performed using the Quantity Tools of Image Lab software (Bio-Rad).

LUC Complementation Imaging Assay

The LCI assay for detecting protein interactions was performed in *N. benthamiana* leaves as described previously (Liu et al., 2017). In brief, full length *SDEL1* and *SPX4* were separately fused with the N- and C-terminal parts of the luciferase reporter gene *LUC* (nLUC and cLUC), generating the vectors *SPX4-nLUC* and *SDEL-cLUC*. The vectors were co-infiltrated into *N. benthamiana* leaves, and the LUC activities were analyzed 48 h after infiltration using NightSHADE LB 985 (Berthold). In total three biological replications were performed with similar results.

GUS Histochemical Analysis

The T1 seeds of *SDEL1pro-gSDEL1-GUS* and *SDEL2pro-gSDEL2-GUS* transgenic plants were grown in standard rice culture solution. The roots and leaves of 14-day-old seedlings were used for GUS analysis as described by Jefferson et al. (1987). The roots and leaves were embedded in 2.5% (w/w) agar and sectioned using a Leica VT 1000 S vibratome. Thin sections (30 μm) were observed under a Leica DM6000M microscope.

Measurement of Pi

Measurements of Pi concentration in plants were performed as described previously (Zhou et al., 2008).

ACCESSION NUMBERS

Sequence data from this article can be found in the database of the Rice Genome Annotation Project under the following accession numbers: SDEL1 (Os12g35320), SDEL2 (Os03g22680), SPX4 (Os03g61200), SPX1 (Os06g40120), PT10 (Os06g21950), PHR2 (Os07g25710), and ACTIN (Os03g50890). Data from this article can be found in the GenBank/EMBL data libraries under accession number NCBI: AY568759 (*OsIPS1*) and the miRNA Database under accession number MI0010490 (*OsmiR827*).

SUPPLEMENTAL INFORMATION

Supplemental Information is available at *Molecular Plant Online*.

FUNDING

This work is dedicated to Ping Wu. This work was funded by grants from the National Key Research and Development Program of China (2016YFD0100705-1), the National Natural Science Foundation of China (31801925, 31772386, and 31601807), and Ningbo Department of Science and Technology (2016C11017). K.Y. was supported by the Innovation Program of Chinese Academy of Agricultural Sciences.

AUTHOR CONTRIBUTIONS

W.R. and M.G. performed most of the described experiments under the supervision of K.Y. X.W. and Z.G. constructed the vectors and purified the proteins. Z.X. performed the subcellular location analysis of SDELs. W.R., M.G., L.X., H.Z., H.S., and C.Y. analyzed the data. K.Y. and W.R. wrote the manuscript. All authors reviewed the manuscript.

ACKNOWLEDGMENTS

No conflict of interest declared.

Received: December 13, 2018
Revised: April 12, 2019
Accepted: April 12, 2019
Published: April 16, 2019

REFERENCES

Bustos, R., Castrillo, G., Linhares, F., Puga, M.I., Rubio, V., Pérez-Pérez, J., Solano, R., Leyva, A., and Paz-Ares, J. (2010). A central regulatory system largely controls transcriptional activation and repression responses to phosphate starvation in *Arabidopsis*. PLoS Genet. **6**:e1001102.

Chen, J.Y., Liu, Y., Ni, J., Wang, Y.F., Bai, Y.H., Shi, J., Gan, J., Wu, Z.C., and Wu, P. (2011). OsPHF1 regulates the plasma membrane localization of low- and high-affinity inorganic phosphate transporters and determines inorganic phosphate uptake and translocation in Rice. Plant Physiol. **157**:269–278.

Ding, S., Zhang, B., and Qin, F. (2015). *Arabidopsis* RZFP34/CHYR1, a ubiquitin E3 ligase, regulates stomatal movement and drought tolerance via SnRK2.6-mediated phosphorylation. Plant Cell **27**:3228–3244.

Duan, K., Yi, K., Dang, L., Huang, H., Wu, W., and Wu, P. (2008). Characterization of a sub-family of *Arabidopsis* genes with the SPX domain reveals their diverse functions in plant tolerance to phosphorus starvation. Plant J. **54**:965–975.

Feng, S., Martinez, C., Gusmaroli, G., Wang, Y., Zhou, J., Wang, F., Chen, L., Yu, L., Iglesias-Pedraz, J.M., Kircher, S., et al. (2008). Coordinated regulation of *Arabidopsis thaliana* development by light and gibberellins. Nature **451**:475–479.

Gilbert, N. (2009). Environment: the disappearing nutrient. Nature **461**:716–718.

Guo, M., Ruan, W., Li, C., Huang, F., Zeng, M., Liu, Y., Yu, Y., Ding, X., Wu, Y., Wu, Z., et al. (2015). Integrative comparison of the role of the PHOSPHATE RESPONSE1 subfamily in phosphate signaling and homeostasis in rice. Plant Physiol. **168**:762–776.

Hamburger, D., Rezzonico, E., MacDonald-Comber Petetot, J., Somerville, C., and Poirier, Y. (2002). Identification and characterization of the *Arabidopsis* PHO1 gene involved in phosphate loading to the xylem. Plant Cell **14**:889–902.

Hiei, Y., Otis, S., Komari, T., and Kumashiro, T. (1994). Efficient transformation of rice (*Oryza sativa L.*) mediated by *Agrobacterium*

and sequence analysis of the boundaries of the T-DNA. Plant J. **6**:271–282.

Hindt, M.N., Akmakjian, G.Z., Pivarski, K.L., Punshon, T., Baxter, I., Salt, D.E., and Guerinot, M.L. (2017). BRUTUS and its paralogs, BTS LIKE1 and BTS LIKE2, encode important negative regulators of the iron deficiency response in *Arabidopsis thaliana*. Metallomics **9**:876–890.

Hu, B., Jiang, Z., Wang, W., Qiu, Y., Zhang, Z., Liu, Y., Li, A., Gao, X., Liu, L., Qian, Y., et al. (2019). Nitrate-NRT1.1B-SPX4 cascade integrates nitrogen and phosphorus signalling networks in plants. Nat. Plants **5**:401–413.

Jefferson, R.A., Kavanagh, T.A., and Bevan, M.W. (1987). GUS fusions: β-glucuronidase as a sensitive and versatile gene fusion marker in higher plants. EMBO J. **6**:3901–3907.

Jung, J., Ried, M., Hothorn, M., and Poirier, Y. (2018). Control of plant phosphate homeostasis by inositol pyrophosphates and the SPX domain. Curr. Opin. Biotechnol. **49**:156–162.

Kant, S., Peng, M., and Rothstein, S.J. (2011). Genetic regulation by NLA and MicroRNA827 for maintaining nitrate-dependent phosphate homeostasis in *Arabidopsis*. PLoS Genet. **7**:e1002021.

Kirkby, E. (2012). Introduction, definition and classification of nutrients. In Marschner's Mineral Nutrition of Higher Plants, 3rd edn, H. Marschner, ed. (London: Academic Press), pp. 3–5.

Lin, W.Y., Lin, Y.Y., Chiang, S.F., Syu, C., Hsieh, L.C., and Chiou, T.J. (2018). Evolution of *microRNA827* targeting in the plant kingdom. New Phytol. **217**:1712–1725.

Lin, W., Huang, T., and Chiou, T. (2013). Nitrogen limitation adaptation, a target of microRNA827, mediates degradation of plasma membrane–localized phosphate transporters to maintain phosphate homeostasis in *Arabidopsis*. Plant Cell **25**:4061–4074.

Liu, F., Wang, Z.Y., Ren, H.Y., Shen, C.J., Li, Y., Ling, H.Q., Wu, C.Y., Lian, X.M., and Wu, P. (2010). OsSPX1 suppresses the function of OsPHR2 in the regulation of expression of OsPT2 and phosphate homeostasis in shoots of rice. Plant J. **62**:508–517.

Liu, J., Cheng, X., Liu, P., Li, D., Chen, T., Gu, X., and Sun, J. (2017). MicroRNA319-regulated TCPs interact with FBHs and PFT1 to activate CO transcription and control flowering time in *Arabidopsis*. PLoS Genet. **13**:e1006833.

Liu, J., Yang, L., Luan, M., Wang, Y., Zhang, C., Zhang, B., Shi, J., Zhao, F.G., Lan, W., and Luan, S. (2015). A vacuolar phosphate transporter essential for phosphate homeostasis in *Arabidopsis*. Proc. Natl. Acad. Sci. U S A **112**:E6571–E6578.

Liu, T., Huang, T., Tseng, C., Lai, Y., Lin, S., Lin, W., Chen, J., and Chiou, Z. (2012). PHO2-dependent degradation of PHO1 modulates phosphate homeostasis in *Arabidopsis*. Plant Cell **24**:2168–2183.

Liu, T., Huang, T., Yang, S., Hong, Y., Huang, S., Wang, F., Chiang, S., Tsai, S., Lu, W., and Chiou, T. (2016). Identification of plant vacuolar transporters mediating phosphate storage. Nat. Commun. **7**:11095.

Lv, Q., Zhong, Y., Wang, Y., Wang, Z., Zhang, L., Shi, J., Wu, Z., Liu, Y., Mao, C., Yi, K., et al. (2014). SPX4 negatively regulates phosphate signaling and homeostasis through its interaction with PHR2 in rice. Plant Cell **26**:1586–1597.

Ma, X., Zhang, Q., Zhu, Q., Liu, W., Chen, Y., Qiu, R., Wang, B., Yang, Z., Li, H., Lin, Y., et al. (2015). A robust CRISPR/Cas9 system for convenient, high-efficiency multiplex genome editing in monocot and dicot plants. Mol. Plant **8**:1274–1284.

Manning, D.A.C. (2008). Phosphate minerals, environmental pollution and sustainable agriculture. Elements **4**:105–108.

Mao, Y., Zhang, H., Xu, N., Zhang, B., Gou, F., and Zhu, J. (2013). Application of the CRISPR-Cas system for efficient genome engineering in plants. Mol. Plant **6**:2008–2011.

Marino, D., Froidure, S., Canonne, J., Ben Khaled, S., Khafif, M., Pouzet, C., Jauneau, A., Roby, D., and Rivas, S. (2013). *Arabidopsis* ubiquitin ligase MIEL1 mediates degradation of the transcription factor MYB30 weakening plant defence. Nat. Commun. **4**:1476.

Morris, K., Thornber, S., Codrai, L., Richardson, C., Craig, A., Sadanandom, A., Thomas, B., and Jackson, S. (2010). DAY NEUTRAL FLOWERING represses CONSTANS to prevent arabidopsis flowering early in short days. Plant Cell. **22**:1118–1128.

Neumann, G., and Römheld, V. (2012). Rhizosphere chemistry in relation to plant nutrition. In Marschner's Mineral Nutrition of Higher Plants, 3rd edn, H. Marschner, ed. (London: Academic Press), pp. 347–368.

Poirier, Y., Thoma, S., Somerville, C., and Schiefelbein, J. (1991). Mutant of *Arabidopsis* deficient in xylem loading of phosphate. Plant Physiol. **97**:1087–1093.

Puga, M.I., Mateos, I., Charukesi, R., Wang, Z., Franco-Zorrilla, J.M., de Lorenzo, L., Irigoyen, M.L., Masiero, S., Bustos, R., Rodríguez, J., et al. (2014). SPX1 is a phosphate-dependent inhibitor of phosphate starvation response 1 in *Arabidopsis*. Proc. Natl. Acad. Sci. U S A **111**:14947–14952.

Ren, F., Guo, Q.Q., Chang, L.L., Chen, L., Zhao, C.Z., Zhong, H., and Li, X.B. (2012). Brassica napus PHR1 gene encoding a MYB-like protein function in response to phosphate starvation. PLoS One **7**:e44005.

Ruan, W., Guo, M., Wu, P., and Yi, K. (2017). Phosphate starvation induced OsPHR4 mediates Pi-signaling and homeostasis in rice. Plant Mol. Biol. **93**:327–340.

Rubio, V., Linhares, F., Solano, R., Martín, A.C., Iglesias, J., Leyva, A., and Paz-Ares, J. (2001). A conserved MYB transcription factor involved in phosphate starvation signaling both in vascular plants and in unicellular algae. Genes Dev. **15**:2122–2133.

Secco, D., Wang, C., Arpat, B.A., Wang, Z., Poirier, Y., Tyerman, S.D., Wu, P., Shou, H., and Whelan, J. (2012a). The emerging importance of the SPX domain-containing proteins in phosphate homeostasis. New Phytol. **193**:842–851.

Secco, D., Wang, C., Shou, H., and Whelan, J. (2012b). Phosphate homeostasis in the yeast *Saccharomyces cerevisiae*, the key role of the SPX domain-containing proteins. FEBS Lett. **586**:289–298.

Shen, Q., Liu, Z., Song, F., Xie, Q., Hanley-Bowdoin, L., and Zhou, X. (2011). Tomato SlSnRK1 protein interacts with and phosphorylates bC1, a pathogenesis protein encoded by a geminivirus b-satellite. Plant Physiol. **157**:1394–1406.

Shi, J., Hu, H., Zhang, K., Zhang, W., Yu, Y., Wu, Z., and Wu, P. (2014). The paralogous SPX3 and SPX5 genes redundantly modulate Pi homeostasis in rice. J. Exp. Bot. **65**:859–870.

Stone, S.L., Hauksdóttir, H., Troy, A., Herschleb, J., Kraft, E., and Callis, J. (2005). Functional analysis of the RING-type ubiquitin ligase family of *Arabidopsis*. Plant Physiol. **137**:13–30.

Valdés-López, O., Arenas-Huertero, C., Ramírez, M., Girard, L., Sánchez, F., Vance, C.P., Luis Reyes, J., and Hernández, G. (2008). Essential role of MYB transcription factor: PvPHR1 and microRNA: *PvmiR399* in phosphorus-deficiency signaling in common bean roots. Plant Cell Environ. **31**:1834–1843.

Walter, M., Chaban, C., Schütze, K., Batistic, O., Weckermann, K., Näke, C., Blazevic, D., Grefen, C., Schumacher, K., Oecking, C., et al. (2004). Visualization of protein interactions in living plant cells using bimolecular fluorescence complementation. Plant J. **40**:428–438.

Wang, C., Huang, W., Ying, Y., Li, S., Secco, D., Tyerman, S., Whelan, J., and Shou, H. (2012). Functional characterization of the rice SPX-MFS family reveals a key role of OsSPX-MFS1 in controlling phosphate homeostasis in leaves. New Phytol. **196**:139–148.

Wang, J., Sun, J., Miao, J., Guo, J., Shi, M., Chen, Y., Zhao, X., Li, B., Han, F., Tong, Y., et al. (2013). A phosphate starvation response regulator Ta-PHR1 is involved in phosphate signaling and increases grain yield in wheat. Ann. Bot. (Lond). **111**:1139–1153.

Wang, Z., Ruan, W., Shi, J., Zhang, L., Xiang, D., Yang, C., Li, C., Wu, Z., Liu, Y., Yu, Y., et al. (2014). Rice SPX1 and SPX2 inhibit phosphate starvation responses through interacting with PHR2 in a phosphate-dependent manner. Proc. Natl. Acad. Sci. U S A **111**:14953–14958.

Wild, R., Gerasimaite, R., Jung, J.Y., Truffault, V., Pavlovic, I., Schmidt, A., Saiardi, A., Jessen, H.J., Poirier, Y., Hothorn, M., et al. (2016). Control of eukaryotic phosphate homeostasis by inositol polyphosphate sensor domains. Science **352**:986–990.

Yang, J., Wang, L., Mao, C., and Lin, H. (2017). Characterization of the rice NLA family reveals a key role for OsNLA1 in phosphate homeostasis. Rice (N. Y). **10**:52.

Ye, Q., Wang, H., Su, T., Wu, W.H., and Chen, Y.F. (2018). The ubiquitin E3 ligase PRU1 regulates WRKY6 degradation to modulate phosphate homeostasis in response to low-Pi stress in *Arabidopsis*. Plant Cell. **30**:1062–1076.

Yoshida, S., Forno, D.A., Cock, J.H., and Gomez, K.A. (1976). Laboratory Manual for Physiological Studies of Rice, 3rd edn (Manila, The Philippines: International Rice Research Institute).

Yue, W., Ying, Y., Wang, C., Zhao, Y., Dong, C., Whelan, J., and Shou, H. (2017). OsNLA1, a RING-type ubiquitin ligase, maintains phosphate homeostasis in *Oryza sativa* via degradation of phosphate transporters. Plant J. **90**:1040–1051.

Zhong, Y., Wang, Y., Guo, J., Zhu, X., Shi, J., He, Q., Liu, Y., Wu, Y., Zhang, L., Lv, Q., et al. (2018). Rice SPX6 negatively regulates the phosphate starvation response through suppression of the transcription factor PHR2. New Phytol. **219**:135–148.

Zhou, J., Jiao, F., Wu, Z., Li, Y., Wang, X., He, X., Zhong, W., and Wu, P. (2008). OsPHR2 is involved in phosphate-starvation signaling and excessive phosphate accumulation in shoots of plants. Plant Physiol. **146**:1673–1686.